Wiley Online Library Early View publication on www.wileyonlinelibrary.com (issue and page numbers not yet assigned; citable using Digital Object Identifier – DOI)

J. Biophotonics 1–9 (2014) / **DOI** 10.1002/jbio.201400070

Journal of BIOPHOTONICS

Full Article

Ultra-sensitive immunoassay biosensors using hybrid plasmonic-biosilica nanostructured materials

Jing Yang[1], *Le Zhen*[2], *Fanghui Ren*[1], *Jeremy Campbell*[2], *Gregory L. Rorrer**[,2], *and Alan X. Wang**[,1]

[1] School of Electrical Engineering and Computer Science, Oregon State University, Corvallis, OR, 97331, USA
[2] School of Chemical, Biological & Environmental Engineering, Oregon State University, Corvallis, OR, 97331, USA

Received 26 Juny 2014, revised 12 August 2014; 5 September 2014, accepted 8 September 2014
Published online 26 September 2014

Key words: immunoassay, surface-enhanced Raman scattering, diatom biosilica, photonic crystal, surface plasmon

We experimentally demonstrate an ultra-sensitive immunoassay biosensor using diatom biosilica with self-assembled plasmonic nanoparticles. As the nature-created photonic crystal structures, diatoms have been adopted to enhance surface plasmon resonances of metal nanoparticles on the surfaces of diatom frustules and to increase the sensitivity of surface-enhanced Raman scattering (SERS). In this study, a sandwich SERS immunoassay is developed based on the hybrid plasmonic-biosilica nanostructured materials that are functionalized with goat anti-mouse IgG. Our experimental results show that diatom frustules improve the detection limit of mouse IgG to 10 pg/mL, which is ~100× better than conventional colloidal SERS sensors on flat glass.

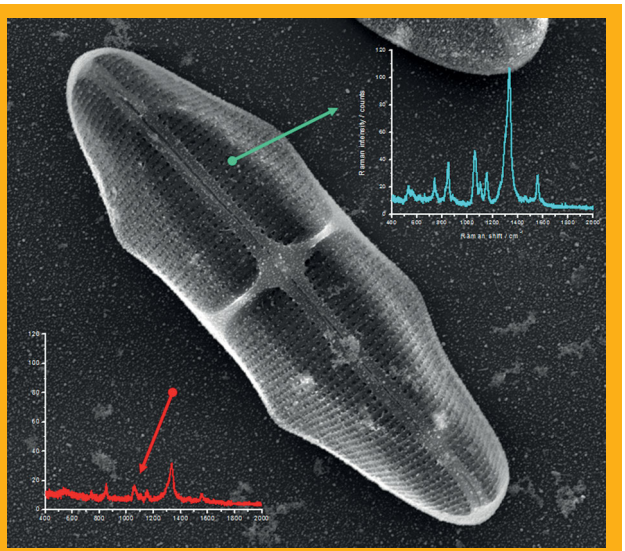

Ultra-sensitive immunoassay biosensor using diatom biosilica with self-assembled plasmonic nanoparticles.

1. Introduction

Immunoassay based on specific recognition between an antigen and a complementary antibody has become an essential and reliable tool for clinical diagnosis and disease detection in recent years [1, 2]. A large number of immunoassay readout techniques have been developed in the past few decades, including optical [3–6], electrical [7], and mass measurement methods [8]. Among these techniques, fluorescence-based immunoassay has been most widely used; however, it suffers moderate sensitivity, concerns of photo-bleaching, and limited multiplex detection capability due to the broad fluorescence band [9]. As an alternative detection method, a surface-enhanced Raman scattering (SERS) based

* Corresponding authors: e-mail: rorrergl@engr.orst.edu, wang@eecs.oregonstate.edu

immunoassay was first reported in 1989 by Tarcha et al. [10]. Since then, SERS has attracted significant research interest due to its high detection sensitivity [11, 12], narrow spectral bandwidth for multiplex detection [13–15], immunity to photo-bleaching [16], and fingerprint information of various molecules. Typically, SERS-based immunoassays are implemented on colloidal gold nanoparticles (Au NPs) or silver nanoparticles (Ag NPs) that are coated on flat glass substrates. Although inexpensive and easy to be functionalized, the sensitivity of such simple chemically-prepared sensors cannot meet the stringent requirement of many biomedical applications.

In recent years, rationally designed optical biosensors [17–20] have demonstrated unprecedented detection sensitivity, reproducibility, reliability, and specificity compared with conventional colloidal plasmonic sensors. For example, photonic crystals [21, 22] can increase the local field intensities and lead to additional Raman enhancement to improve the detection limit. However, the high cost of fabricating nanophotonic devices and the difficulty of coupling light into rationally designed nanosensors have prohibited their applications in point-of-care testing and as disposable sensors. Fortunately, Mother Nature provides many resources of photonic-crystal-like materials without using complex and expensive nanofabrication techniques. Diatom frustules possess hierarchical nano-scale features consisting of two dimensional (2-D) periodic pores. Our previous studies proved that such unique photonic crystal features are capable of enhancing localized surface-plasmon resonances of self-assembled metal NPs on the surface of diatom frustules, which will significantly enhance the Raman signals of the molecules adsorbed to the nanoparticle surfaces [23].

In this paper, we exploit the enhanced SERS sensitivity of the hybrid plasmonic-biosilica nanostructured materials to detect the immune reactions between antigens and antibodies. We developed a novel SERS-based sandwich immunoassay using hybrid plasmonic-biosilica nanostructured materials. In this immunoassay, Ag NPs were self-assembled onto the diatom frustules and then functionalized with model antibody – goat anti-mouse IgG. The selectivity to detect specific antigens were tested by challenging the immunoassay sensors with complementary antigen (mouse IgG) and non-comlementary antigen (human IgG), respectively. Finally, we quantitatively compared the detection limit of the SERS immunoassays on diatom biosilica and on glass substrates. The contribution of diatom frustules to the enhanced sensitivity was verified by the SERS mapping images. To the best of our knowledge, this is the first report of a SERS-based immunoassay sensor based on photonic crystal platforms.

2. Experimental

2.1 Reagents

The antibody (goat anti-mouse IgG) and antigens (mouse IgG and human IgG) utilized for the sandwich assay were obtained from Pierce. Bovine serum albumin (BSA), aminopropyltriethoxylsilane (APTES) and 5,5′-dithiobis (2-nitrobenzoic acid) (DTNB) were purchased from Sigma-aldrich. Hydrogen tetrachloroaurate (III) and silver nitrate were purchased from Alfa Aesar. Trisodium citrate was purchased from Macron chemicals. All chemicals and materials used without further notice were analytical grade and used as received. Deionized (DI) water (18.1 MΩ cm) was used throughout the experiment.

2.2 Preparation of diatom biosilica substrates

Diatoms (*Pinnularia sp.*) were prepared by traditional microbiological cultivation [24]. The diatoms were harvested and cleaned by hydrogen peroxide and hydrogen chloride in order to remove organic materials in diatoms. The diatoms were then weighed and redispersed in ethanol at a concentration of 0.1 mg/mL. Glass slides were cleaned in an ultrasonic bath with DI water and ethanol respectively, each for 10 min. The glass slides were then coated with 200 μL of diatom ethanol solution. After drying, the glass slides decorated with diatom frustules were loaded into an annealing furnace and annealed at 450 °C for 1 h to improve the adhesion of diatom frustules on glass slides, as shown in Figure 1. After that, the prepared substrates were ready for future functionalization after cooling down.

2.3 Preparation of SERS-active immune substrate

The characteristic features of diatom frustules are the bio-mineralized cell walls, which consist of amorphous silica. Diatom frustules can be easily functionalized with metal NPs and biomolecules, and therefore replace the role of glass slides in immunoassay with additional SERS enhancement factors. The surface silanol groups on diatom frustules were first functionalized with amine groups by APTES, as shown in Figure 1. Briefly, the glass substrates with diatom frustules were immersed into 50.0 mL anhydrous ethanol, and 50 μL of APTES solution was

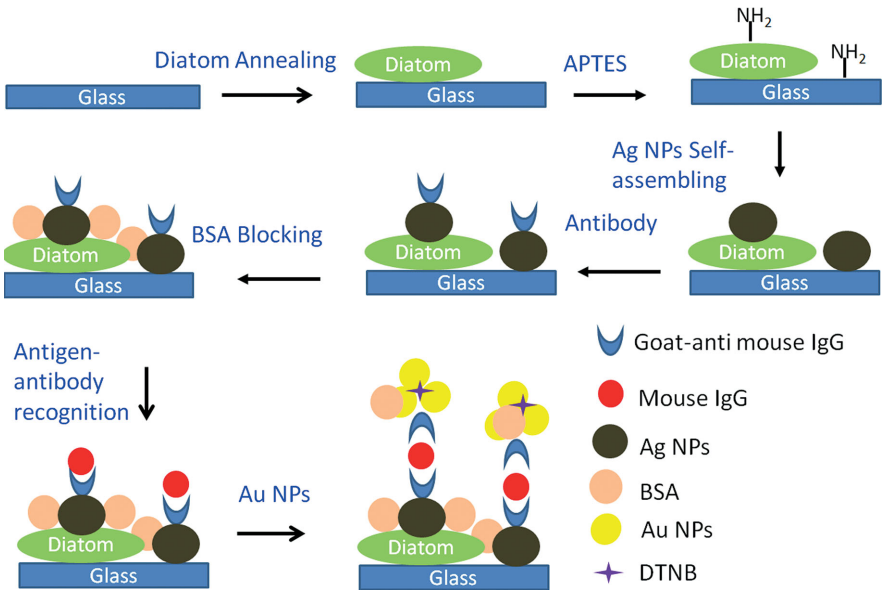

Figure 1 Schematic diagram of the SERS immunoassay using diatom biosilica with self-assembled Ag NPs.

added into the ethanol solution. The reaction was heated to 50 °C for 1 h. The substrates were then rinsed with ethanol and DI water three times to remove excessive APTES. Ag NPs were synthesized according to the method reported by Lee and Meisel with a surface plasmon resonance (SPR) peak at 405 nm [25], as shown in Figure S1. In our design, Ag NPs have two roles: one is to provide fundamental SERS enhancement; the other one is to serve as the substrates for antibody attachment. The Ag NPs were self-assembled onto the surfaces of diatoms by immersing the glass slides with diatoms into 30 mL of Ag NP solution for 1 h. Ag NPs were self-assembled onto the surfaces of the positive-charge-modified diatom frustules and the surrounding glass slides by electrostatic interactions. After being rinsed with DI water three times, the substrates with self-assembled Ag NPs were functionalized with antibody. Briefly, 20 µL of goat anti-mouse IgG (1 mg/mL in phosphate buffered saline (PBS)) were pipetted onto the substrates and incubated at 4 °C in a moist chamber for overnight allowing the adsorption of proteins onto Ag NPs through thiol groups as well as ionic, hydrophilic and hydrophobic interactions [26]. Then the antibody-functionalized substrate was rinsed with DI water to remove unadsorbed antibody molecules and dried by gentle nitrogen gas. To reduce the non-specific binding of the immunoassay, the nonspecific adsorption sites on the surfaces of Ag NPs were blocked with BSA solution (20 µL of 3% BSA in PBS) for 2 h at room temperature. The substrates were then thoroughly rinsed with DI water and dried by gentle nitrogen gas. The antibody immobilized diatom substrates were stored at 4 °C for future test.

2.4 Preparation of the DTNB-labeled immuno-Au NPs

Au NPs were synthesized according to the method reported by Lee and Meisel [25] with a SPR peak at 523 nm as shown in Figure S2. The DTNB-labeled Au NPs were prepared by adding 10 µL of DTNB ethanol solution (1 mM) to 1 mL of raw Au NPs and incubated under continuous stirring at 100 rpm for overnight. DTNB, a strongly Raman-active reporter, was used to label Au NPs and introduce Raman signals. During the interaction with Au NPs, a DTNB molecule was bisected into two TNB molecules, which were spontaneously adsorbed onto the surfaces of Au NPs via the thiol groups of TNB molecules. The DTNB labeled Au NPs were then centrifuged at 9,000 rpm for 25 min two times to remove the residual DTNB molecules. The supernatant was discarded and the sediment was finally re-suspended in 1 mL diluted PBS (mixture of 200 µL of PBS and 800 µL of DI water). The color of Au NPs turned from wine red to navy blue indicating the formation of Au NPs aggregates. The SPR peak of Au NPs red shifted from 523 nm to 540 nm (Figure S2), which also confirmed the formation of Au NP aggregates. When compared with mono-dispersed Au NPs, Au NP aggregates functionalized with antibodies and Raman reporters were introduced to provide stronger SERS enhancement [27]. To immobilize the DTNB labeled Au NPs, 20 µL of goat-anti mouse IgG (1 mg/mL) was added into the Au NPs and then incubated at room temperature for 1 h. The antibody-functionalized Au NPs were collected by centrifugation at 7,000 rpm for 20 min. The sediment

was re-suspended in 1 mL of DI water. Then the DTNB-labeled immuno-Au NPs were blocked by BSA (30 μL of 3% BSA in PBS) to shield the unconjugated sites on Au NPs and incubated at room temperature for another 1 h. Finally, the DTNB-labeled immuno-Au NPs were centrifuged and re-suspended in 1 mL of DI water. The prepared DTNB-labeled immuno-Au NPs were preserved at 4 °C before being used.

2.5 Immunoassay protocol

Our SERS-based immunoassay biosensing procedure is similar to a standard sandwich protocol of the enzyme-linked immunosorbent assay (ELISA), as shown in Figure 1. Typically, 20 μL of antigen were pipetted onto each spot with immobilized goat anti-mouse IgG antibody on the SERS-active immune substrate that is prepared in Section 2.3. The immobilization of the antigen was visualized by introducing Fluorescein isothiocyanate (FITC)-labeled mouse IgG as shown in Figure S3. To test the specificity of the immuno-complex, the hybrid plasmonic-biosilica, which is functionalized by goat anti-mouse IgG, was challenged by complementary mouse IgG and no-complementary human IgG. After 2 h immune recognition at room temperature, the substrate was rinsed with DI water, and dried by gentle nitrogen gas. 20 μL of DTNB-labeled immuno-Au NPs prepared in section 2.4 were pipetted onto each antigen immobilized spot and incubated at room temperature for 1 h. Finally, the immunoassay was rinsed with DI water thoroughly, and dried by gentle nitrogen gas for future Raman spectra and mapping test.

2.6 Instrumentation

Bare diatom frustules, Ag NPs self-assembled diatom frustules, and diatom frustule biosilica immunoassay with DTNB-labeled immune Au NPs were imaged by scanning electronic microscopy (SEM). The optical absorption spectra of Ag NPs, Au NPs and DTNB-labeled immune Au NPs were characterized by UV-vis extinction spectroscopy. SERS measurements including Raman line scans and maps were acquired with a Horiba Jobin Yvon Lab Ram HR 800 Raman microscope. All the samples were excited with a 2.0 mW, 785 nm incident laser excitation source through a 100 × (0.9 N.A.) objective lens, which was manually focused to obtain the highest Raman signal intensity. The laser spot size is 2 μm in diameter. The confocal pinhole was set to a diameter of 100 μm, which minimized the background signals and maximized the sample signals that were collected by a CCD camera with a 1200 lines mm^{-1} grating. Raman spectra were acquired with 1 s integration time in the Raman spectral range from 400 cm^{-1} to 2000 cm^{-1}. Raman mapping images were obtained with a 10 × 10 point mapping array. They were collected using the DuoScan module, with a 3.0 μm step size, 100 s accumulation time, and collected in the Raman spectral range from 1000 cm^{-1} to 1500 cm^{-1}. Each spectrum was based on the average spectrum of 20 measurements of different spots of 20 different diatoms for each sample. Spectra were recorded and processed with Horiba LabSpec 5 data acquisition and analysis software, which was used for spectra baseline subtraction.

3. Results and discussion

3.1 Characterization of hybrid plasmonic-biosilica immunoassay

In this study, *Pinnularia sp*. was chosen as the model diatom. The frustule of this specie possesses periodic ordered array at two scales: a rectangular lattice of 200–400 nm pores at the sub-micron scale and a concentric array of fine features lining the base of each pore at sub-100 nm scale [24]. The SEM images presented in Figure 2A and B show a representative

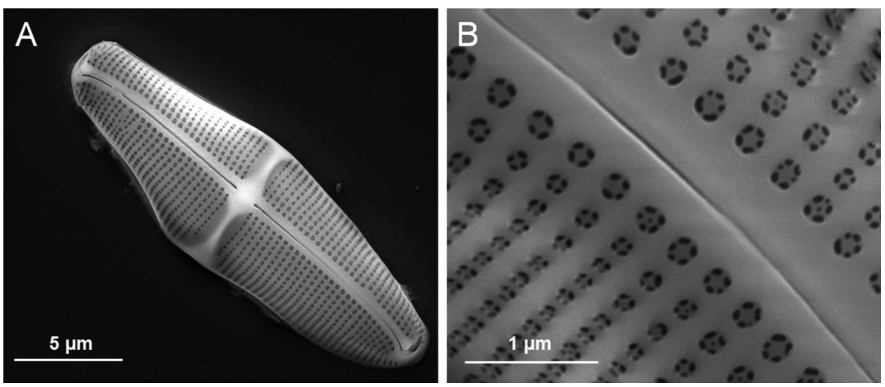

Figure 2 SEM images of a single diatom frustule and its fine features.

diatom frustule and its fine features, respectively. The length of the diatom frustule is around 15–20 μm. Diatom frustules also exhibit unique plum flower shaped sub-pores with diameters from 50 nm to 80 nm. The periodic sub-micron scale pore structures of diatom frustules enable guided-mode resonances (GMRs) at visible wavelengths, which are similar to artificial photonic crystals [28, 29]. Next, we will utilize these natural photonic crystals, diatom biosilica, to enhance the SERS sensitivity for immunoassay sensing.

3.2 *Experimental results of the SERS immuno-sensing*

Figure 3A shows the bright field optical image of a typical diatom frustule with self-assembled Ag NPs. To validate the enhanced SERS sensitivity by diatom frustules when compared with glass substrates, the SERS mapping image of 1 mM pure DTNB on the diatom frustule as well as the surrounding glass substrate is shown in Figure 3B. DTNB provides an intense Raman peak at 1331 cm^{-1}, which is assigned to the symmetric stretch of the nitro group [30]. The SERS mapping image was decoded using the integrated peak intensity at 1320–1340 cm^{-1}. Diatom frustules showed much stronger SERS signals from DTNB than glass slides did. The measurement confirms that 4× stronger Raman signals can be achieved on diatom frustules as the SERS substrate. Our previous theoretical and experimental study have demonstrated that diatom frustules can be utilized as an integration platform to enhance localized SPR of self-assembled Ag NPs on the surface of diatom frustules. The SERS enhancement introduced by diatom frustules is attributed to the couplings between localized surface plasmons (LSPs) of Ag NPs and the GMRs of diatom frustules [23].

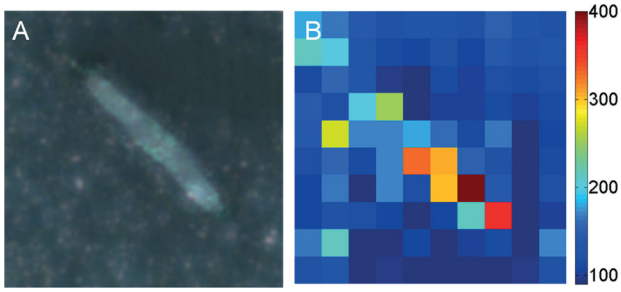

Figure 3 Bright-field image of a diatom frustule (**A**) and Raman mapping image of free DTNB (**B**) on a single diatom frustule.

The SEM image in Figure 4A verifies that Ag NPs have been successfully self-assembled onto the surfaces of diatom frustules. Figure 1 shows the procedure of our SERS immunoassay using the hybrid plasmonic-biosilica. In this immunoassay, the antibody, goat-anti-mouse IgG, was immobilized onto the surface of Ag NPs, then exposed to antigens, followed by exposure to Au NPs functionalized by DTNB and the antibody, which is similar to a standard ELISA protocol. The concentrations of the complementary antigen, mouse IgG, vary from 10 μg/mL to 1 pg/mL. In order to test the immunocomplex specificity, our immunoassay was also challenged by non-complementary human IgG at a concentration of 10 μg/mL. As it is well known, the antigen acts as an amplifier, and targets antibody-conjugated Au NP aggregates. More mouse IgG molecules will capture a larger number of Au NP aggregates conjugated with goat-anti mouse IgG. It is confirmed by the SEM images in Figure 4B and C. Figure 4B and C show a sparse and a dense distribution of Au NP aggregates at an antigen concentration of 1.0×10^{-10} g/mL and 1.0×10^{-7} g/mL, respectively. Denser distributions of DTNB-functionalized Au NPs are expected to provide stronger SERS signals.

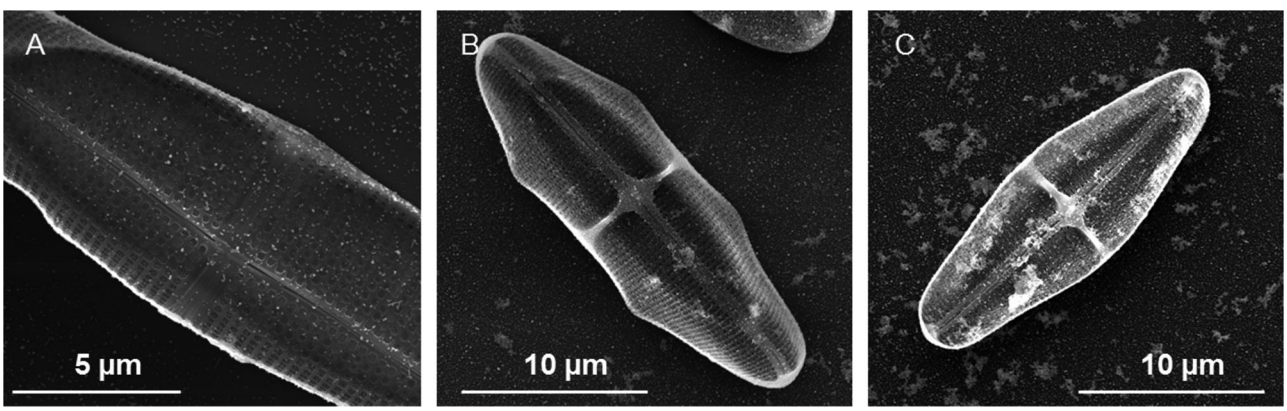

Figure 4 SEM images of a diatom frustule with self-assembled Ag NPs (**A**), and the hybrid plasmonic-biosilica immunoassay with mouse IgG at 1.0×10^{-10} g/mL (**B**) and 1.0×10^{-7} g/mL (**C**).

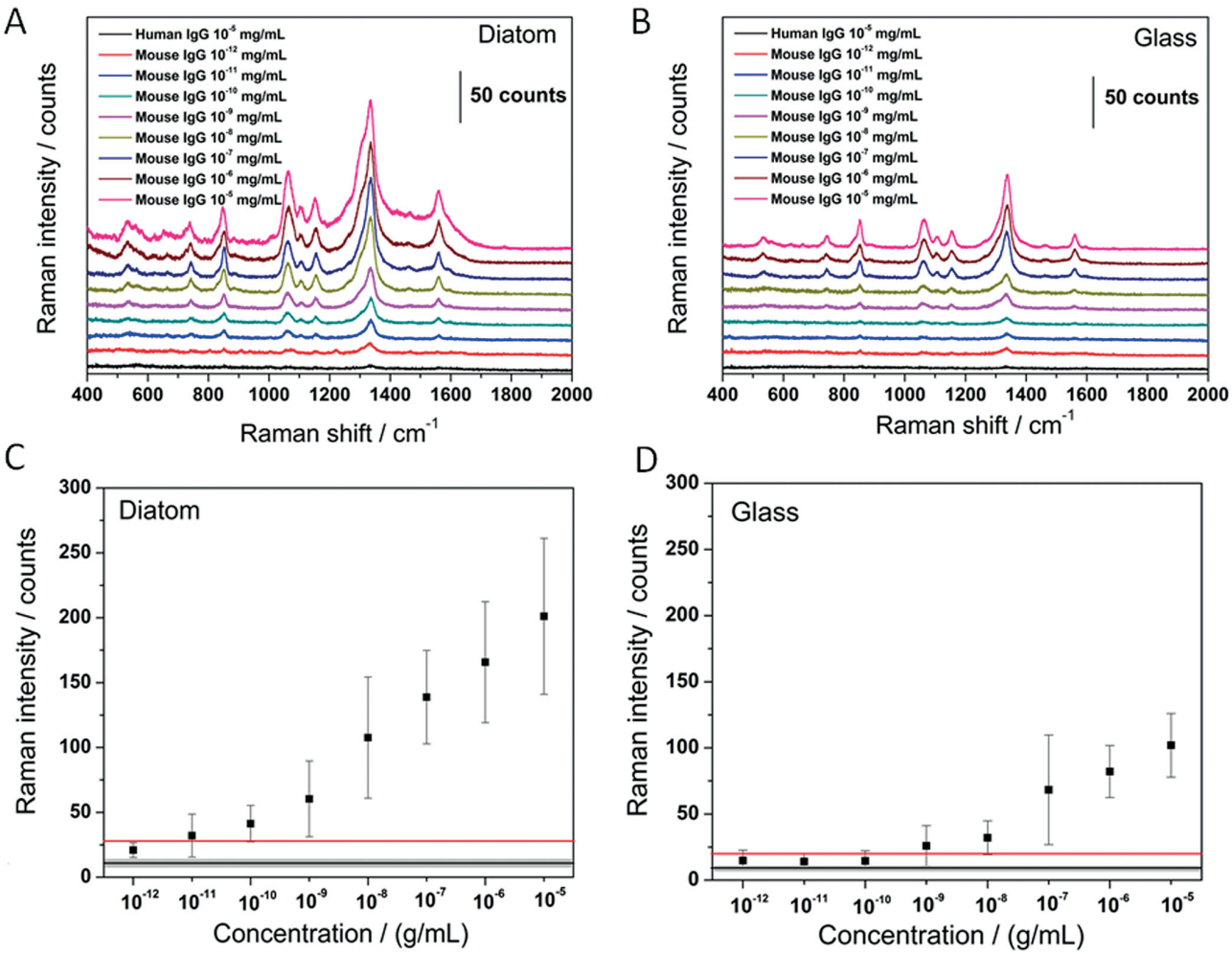

Figure 5 SERS spectra, offset for clarity, acquired at mouse IgG concentration from 10 µg/mL to 1 pg/mL on diatoms frustules (**A**) and on glass slides (**B**). Dose-response curves of the Raman peaks at 1331 cm^{-1} acquired from the SERS spectra on diatom frustules (**C**) and glass slides (**D**). (Average SERS intensities and error bars of human IgG at 10 µg/mL on diatom frustules and on glass slides were indicated as the solid lines and gray ribbon in (**C**) and (**D**), and the detection limit on diatom frustules and on glass slides were indicated as the red line in (**C**) and (**D**)).

The immunoassay sensing results of the antigens are shown in Figure 5. Figure 5A shows the SERS spectra of DTNB on diatom frustules with different antigen concentrations. Each spectrum represents the average measurement results of 20 randomly selected spots on diatom frustules. The intensity of the SERS signals of the DTNB-labeled immunoassay shows a strong correlation with the concentration of mouse IgG, which is consistent with the SEM images of the densities of Au NPs in Figure 4 B and C. For non-complementary antigen detection (the black curve in Figure 5A), the immunoassay that is challenged by 10 µg/mL human IgG exhibits the lowest DTNB SERS signals. For complementary antigen detection, even at a low concentration of 1 pg/mL mouse IgG, the SERS spectrum is still much more prominent than that from 10 µg/mL human IgG. Our experimental results prove that our immunoassay has excellent detection specificity and sensitivity.

A more quantitative analysis of our results is presented in Figure 5C. This curve was obtained by plotting the most prominent Raman peak of DTNB at 1331 cm^{-1} with respect to different mouse IgG concentrations. The curve shows a nearly linear dependence of the Raman signal intensity of DTNB at 1331 cm^{-1} vs. the log-scale concentrations of mouse IgG from 100 pg/mL to 10 µg/mL. Below 100 pg/mL mouse IgG concentration, the SERS signals gradually saturate and approach a constant level, which is possibly due to the non-specific binding of the Au NP aggregates to the immunoassay. For non-complementary detection, human IgG at 10 µg/mL shows very low SERS intensity as indicated by the grey-scale bar (average signal with standard deviation) in Figure 5C. Therefore, the experimental results prove

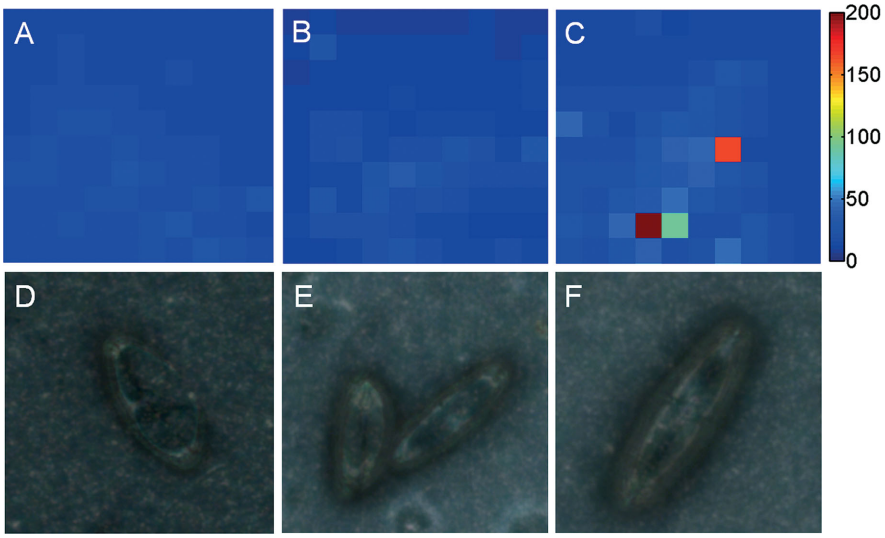

Figure 6 Bright field optical images and Raman mapping images of the hybrid plasmonic-biosilica immunoassay with human IgG at 10 μg/mL (**A**, **D**), mouse IgG at 1 pg/mL (**B**, **E**), and mouse IgG at 10 pg/mL (**C**, **F**).

that the hybrid plasmonic-biosilica immunoassay can provide high selectivity to detect complementary antigens at ultra-low concentration.

We also compared the SERS immunoassay on conventional glass slides by collecting the SERS spectra on the flat glass area surrounding the diatom frustules of the same immunoassay, as shown in Figure 5B and D. The immune-sensing results on glass substrates show much weaker SERS signals than on diatom frustules. In addition, the SERS signals start to saturate when the mouse IgG concentration drops to 1 ng/mL. When the concentration of mouse IgG decreases below 100 pg/mL, the Raman intensities at 1331 cm^{-1} become completely constant and are very close to the SERS signals from human IgG, which makes it difficult to detect.

Mapping results of the Raman signals visualized the selective recognition of the adsorbed antigens, as shown in Figure 6. The significant enhancement of the Raman signals for the detection of mouse IgG on diatom frustules is clearly shown in the Raman mapping images. In Figure 6B and E, the morphology of the two diatom frustules can be identified from the surrounding glass substrate even at a low mouse IgG concentration of 1 pg/mL. With the increase of the mouse IgG concentration in Figure 6C and F, the mapped Raman signals become stronger. The average intensity ratios of SERS signals from diatom to that from flat glass slides in the mapping images in Figure 6A, B, and C are 1.13, 1.63, and 2.49, respectively. Moreover, there are a few red pixels in the mapping image within the diatom frustule, indicating ultra-strong "hot spots". However in Figure 6A and D, we are not able to observe any enhanced Raman signal for the non-complementary antigen from the diatom frustule. The Raman mapping images of the hybrid plasmonic-biosilica immunoassay agree very well with the previous SERS spectra characterizations.

3.3 Discussion of the detection limit

The detection limit is determined by the nonspecific adsorption of the labeled Au NP aggregates, and is defined as the concentration of mouse IgG that generates signal intensity that is equal to the background signal plus three times of the standard deviation of the background signals [11, 31]. In our study, we used non-complementary antigen, human IgG, as the nonspecific control, and the SERS signals from 10 μg/mL human IgG were used to define the background signals. According to the definition of detection limit, the threshold values of the SERS signals on diatom frustules and flat glass substrates are 27.5 and 20.2 photon counts, respectively, as shown by the red lines in Figure 5C and D (statistic information of the SERS signals is provided in Table S1). Therefore, the detection limits of mouse IgG on diatom frustules and flat glass substrates are 10 pg/mL and 1 ng/mL, respectively. The 100× improvement of the detection limit on diatom frustules is attributed to two factors according to our quantitative measurement results in Figure 5: First, the absolute intensity of the SERS signals on diatom frustules is 2× higher than that on flat glass substrates; Second, the SERS signals on the glass substrates saturate to the threshold value at around 1 ng/ML, while the SERS signals on diatom frustules show positive correlation with the mouse IgG concentration even at 1 pg/mL level. More in-depth understanding of the mechanism of the greatly enhanced sensitivity will be the goal of our future research.

4. Conclusion

In summary, we have successfully demonstrated ultra-sensitive SERS immunoassay biosensors using

nature-created photonic crystals – diatom biosilica frustules. The experimental results proved that diatoms biosilica can achieve a detection limit down to 10 pg/mL, which is two orders of magnitude better than flat glass substrates. In our immunoassay, highly specific detection of the mouse IgG against human IgG was achieved through surface functionalization of the Ag NPs using goat anti-mouse IgG. Moreover, we also mapped the Raman signals of the immobilized diatom frustules, which showed a strong correlation between the enhancement factors and the morphologies of the diatom frustules. This mapping method provides intuitive images of the high detection sensitivity of the diatom frustules and can effectively eliminate many random factors that can affect the measurement of low concentration antigens. It is expected that the hybrid plasmonic-biosilica nanostructured materials will create a new route to develop ultra-sensitive and low-cost immunoassay biosensors to replace rationally designed optical sensors, which can play significant roles to detect trace amount of cancer biomarkers for early diagnosis.

Acknowledgements A. X. Wang would like to acknowledge Marine Polymer Technologies, Inc. and partial support of the National Institute of Health under grant No. of 9R42ES024023-02 to J. Yang. G. L. Rorrer acknowledges support of this research by the National Science Foundation (NSF) through the Emerging Frontiers in Research and Innovation (EFRI) program, award number 1240488.

Author biographies Please see Supporting Information online.

References

[1] F. Rusmini, Z. Y. Zhong, and J. Feijen, Biomacromolecules **8**, 1775 (2007).
[2] R. M. Lequin, Clinical Chemistry **51**, 2415 (2005).
[3] J. C. Riboh, A. J. Haes, A. D. McFarland, C. R. Yonzon, and R. P. Van Duyne, Journal of Physical Chemistry B **107**, 1772 (2003).
[4] O. Kavanagh, M. K. Estes, A. Reeck, R. M. Raju, A. R. Opekun, M. A. Gilger, D. Y. Graham, and R. L. Atmar, Clinical and Vaccine Immunology **18**, 1187 (2011).
[5] T. Kreisig, R. Hoffmann, and T. Zuchner, Analytical Chemistry **83**, 4281 (2011).
[6] T. Li, E. J. Jo, and M. G. Kim, Chemical Communications **48**, 2304 (2012).
[7] J. Zhuang, T. Cheng, L. Z. Gao, Y. T. Luo, Q. Ren, D. Lu, F. Q. Tang, X. L. Ren, D. L. Yang, J. Feng, J. D. Zhu, and X. Y. Yan, Toxicon **55**, 145 (2010).
[8] J. W. Silzel, B. Cercek, C. Dodson, T. Tsay, and R. J. Obremski, Clinical Chemistry **44**, 2036 (1998).
[9] M. D. Porter, R. J. Lipert, L. M. Siperko, G. Wang, and R. Narayanana, Chemical Society Reviews **37**, 1001 (2008).
[10] T. E. Rohr, T. Cotton, N. Fan, and P. J. Tarcha, Analytical Biochemistry **182**, 388 (1989).
[11] D. S. Grubisha, R. J. Lipert, H. Y. Park, J. Driskell, and M. D. Porter, Analytical Chemistry **75**, 5936 (2003).
[12] H. Chon, S. Lee, S. W. Son, C. H. Oh, and J. Choo, Analytical Chemistry **81**, 3029 (2009).
[13] Z. Y. Wang, S. F. Zong, W. Li, C. L. Wang, S. H. Xu, H. Chen, and Y. P. Cui, Journal of the American Chemical Society **134**, 2993 (2012).
[14] Y. Cui, B. Ren, J. L. Yao, R. A. Gu, and Z. Q. Tian, Journal of Raman Spectroscopy **38**, 896 (2007).
[15] H. Chon, S. Lee, S. Y. Yoon, S. I. Chang, D. W. Lim, and J. Choo, Chemical Communications **47**, 12515 (2011).
[16] B. H. Jun, J. H. Kim, H. Park, J. S. Kim, K. N. Yu, S. M. Lee, H. Choi, S. Y. Kwak, Y. K. Kim, D. H. Jeong, M. H. Cho, and Y. S. Lee, Journal of Combinatorial Chemistry **9**, 237 (2007).
[17] M. Lee, S. Lee, J. H. Lee, H. W. Lim, G. H. Seong, E. K. Lee, S. I. Chang, C. H. Oh, and J. Choo, Biosensors & Bioelectronics **26**, 2135 (2011).
[18] M. Li, S. K. Cushing, J. M. Zhang, S. Suri, R. Evans, W. P. Petros, L. F. Gibson, D. L. Ma, Y. X. Liu, and N. Q. Wu, Acs Nano **7**, 4967 (2013).
[19] S. Tian, Q. Zhou, Z. M. Gu, X. F. Gu, and J. W. Zheng, Analyst **138**, 2604 (2013).
[20] A. J. Haes and R. P. Van Duyne, Journal of the American Chemical Society **124**, 10596 (2002).
[21] S. M. Kim, W. Zhang, and B. T. Cunningham, Applied Physics Letters **93** (2008).
[22] X. B. Xu, D. H. Hasan, L. Wang, S. Chakravarty, R. T. Chen, D. L. Fan, and A. X. Wang, Applied Physics Letters **101** (2012).
[23] F. H. Ren, J. Campbell, X. Y. Wang, G. L. Rorrer, and A. X. Wang, Optics Express **21**, 15308 (2013).
[24] C. Jeffryes, T. Gutu, J. Jiao, and G. L. Rorrer, Acs Nano **2**, 2103 (2008).
[25] P. C. Lee and D. Meisel, Journal of Physical Chemistry **86**, 3391 (1982).
[26] C. C. Lin, Y. M. Yang, Y. F. Chen, T. S. Yang, and H. C. Chang, Biosensors & Bioelectronics **24**, 178 (2008).
[27] C. Y. Song, Z. Y. Wang, R. H. Zhang, J. Yang, X. B. Tan, and Y. P. Cui, Biosensors & Bioelectronics **25**, 826 (2009).
[28] S. Yamanaka, R. Yano, H. Usami, N. Hayashida, M. Ohguchi, H. Takeda, and K. Yoshino, Journal of Applied Physics **103** (2008).
[29] T. Fuhrmann, S. Landwehr, M. El Rharbi-Kucki, and M. Sumper, Applied Physics B-Lasers and Optics **78**, 257 (2004).
[30] Z. Y. Wang, S. F. Zong, H. Chen, H. Wu, and Y. P. Cui, Talanta **86**, 170 (2011).
[31] J. D. Driskell, K. M. Kwarta, R. J. Lipert, M. D. Porter, J. D. Neill, and J. F. Ridpath, Analytical Chemistry **77**, 6147 (2005).

Supporting Information

Additional supporting information may be found in the online version of this article at the publisher's website: doi: http://dx.doi.org/10.1002/lpor.201400070.

Figure S1 UV-vis absorption spectra of Ag NPs.

Figure S2 Au NPs (black) and DTNB and antibody functionalized Au NPs (red).

Figure S3 Fluorescence images of (A) immunoassay before mouse IgG immobilization, (B) fully developed immunoassay after FITC-labeled mouse IgG immobilization.

Table S1 Statistic results of the Raman signal intensity (unit: photon counts) at 1331 cm^{-1} in Figure 5C–D for low antigen concentrations.